ARTICLES

Translational control of the innate immune response through IRF-7

Rodney Colina[1]*, Mauro Costa-Mattioli[1]*, Ryan J. O. Dowling[1], Maritza Jaramillo[1], Lee-Hwa Tai[2], Caroline J. Breitbach[3], Yvan Martineau[1], Ola Larsson[1], Liwei Rong[1], Yuri V. Svitkin[1], Andrew P. Makrigiannis[2], John C. Bell[3] & Nahum Sonenberg[1]

Transcriptional activation of cytokines, such as type-I interferons (interferon (IFN)-α and IFN-β), constitutes the first line of antiviral defence. Here we show that translational control is critical for induction of type-I IFN production. In mouse embryonic fibroblasts lacking the translational repressors 4E-BP1 and 4E-BP2, the threshold for eliciting type-I IFN production is lowered. Consequently, replication of encephalomyocarditis virus, vesicular stomatitis virus, influenza virus and Sindbis virus is markedly suppressed. Furthermore, mice with both *4E-BP1* and *4E-BP2* genes (also known as *Eif4ebp1* and *Eif4ebp2*, respectively) knocked out are resistant to vesicular stomatitis virus infection, and this correlates with an enhanced type-I IFN production in plasmacytoid dendritic cells and the expression of IFN-regulated genes in the lungs. The enhanced type-I IFN response in *4E-BP1*$^{-/-}$ *4E-BP2*$^{-/-}$ double knockout mouse embryonic fibroblasts is caused by upregulation of interferon regulatory factor 7 (*Irf7*) messenger RNA translation. These findings highlight the role of 4E-BPs as negative regulators of type-I IFN production, via translational repression of *Irf7* mRNA.

Virus infection activates a subset of genes encoding cytokines and other antiviral proteins that trigger first the innate immune response and subsequently the adaptive immune response. Type-I interferons (IFN-α and IFN-β) are widely expressed cytokines that constitute the first line of defence against virus infections[1–4]. Although transcriptional control of IFN gene expression has a major role in the activation of the innate immune response, it is not known whether translational control is important for this process. Translational control of gene expression provides the cell with a rapid response to external and internal triggers or cues, without invoking the slower nuclear pathways for mRNA synthesis and transport. In eukaryotes, translational control mostly occurs at the rate-limiting initiation step, during which the small 40S ribosomal subunit is recruited to the mRNA[5]. Ribosome recruitment is facilitated by the 5′-cap structure (m^7GpppN, where N is any nucleotide) present on all nuclear transcribed eukaryotic mRNAs[6]. The cap structure is recognized by eukaryotic initiation factor 4F (eIF4F)[7], which consists of eIF4E, the cap-binding subunit[8], eIF4A, a bidirectional RNA helicase[9], and eIF4GI or eIF4GII, scaffolding proteins that bind directly to eIF4E and eIF4A and bridge the mRNA to the ribosome through interaction with eIF3 (ref. 10).

eIF4F complex assembly is inhibited by the 4E-BP translational repressors[7]. Mammals contain three highly related 4E-BPs that compete with eIF4G for a shared binding site on the convex dorsal surface of eIF4E[11,12]. mTOR-mediated phosphorylation of 4E-BP1 (the best characterized 4E-BP) stimulates translation by dissociating 4E-BPs from eIF4E. Hypophosphorylated 4E-BP1 binds to eIF4E with high affinity, whereas increased phosphorylation decreases its affinity for eIF4E[13].

Because viruses have evolved elaborate strategies to usurp the host translation machinery[14], we wished to study the effect of 4E-BPs on virus infections. To this end, we used mouse embryonic fibroblasts (MEFs) and mice deficient in 4E-BP1 and 4E-BP2.

Virus infection is suppressed in *4E-BP1*$^{-/-}$ *4E-BP2*$^{-/-}$ MEFs

To study the role of 4E-BPs in the cell's response to virus infections *ex vivo*, MEFs derived from *4E-BP1*$^{-/-}$ *4E-BP2*$^{-/-}$ double knockout and wild-type mice were used[15]. The *4E-BP1*$^{-/-}$ *4E-BP2*$^{-/-}$ double knockout MEFs lack all three 4E-BPs, because 4E-BP3 is not expressed in MEFs[16]. MEFs were infected with vesicular stomatitis virus (VSV) at a multiplicity of infection (MOI) of 0.5 plaque-forming units (PFU) per cell and viral protein synthesis was analysed by pulse labelling with [^{35}S]methionine at various times after infection. In wild-type MEFs, synthesis of VSV proteins was first detected at 4 h after infection (Fig. 1a). Notably, in *4E-BP1*$^{-/-}$ *4E-BP2*$^{-/-}$ MEFs, no viral proteins were detected at this, or even later, time points (Fig. 1a). Western blot analysis over the time course of infection demonstrated a robust expression of VSV proteins in wild-type MEFs, but not in *4E-BP1*$^{-/-}$ *4E-BP2*$^{-/-}$ MEFs (Fig. 1b). A VSV-induced cytopathic effect at 10 h after infection was observed only in wild-type MEFs (Fig. 1c). The lack of 4E-BPs resulted in reduced (~700-fold) virus titres (Fig. 1d). These data demonstrate that removing 4E-BPs abrogates VSV propagation. At a higher MOI (5 PFU per cell), the difference in the kinetics of VSV replication in wild-type and *4E-BP1*$^{-/-}$ *4E-BP2*$^{-/-}$ MEFs was less pronounced. In wild-type MEFs, VSV proteins were first detected as early as 2 h after infection, as compared to 4 h after infection in *4E-BP1*$^{-/-}$ *4E-BP2*$^{-/-}$ MEFs (Supplementary Fig. 1A). The VSV-induced shut off of host translation in wild-type MEFs occurred at 5 h after infection, whereas in *4E-BP1*$^{-/-}$ *4E-BP2*$^{-/-}$ MEFs, the reduction of cellular translation was barely detectable at 6 h after infection. In agreement with these data, the lack of 4E-BPs resulted in a decrease in infectious virus production (Supplementary Fig. 1B).

To confirm that the VSV-resistant phenotype observed in the *4E-BP1*$^{-/-}$ *4E-BP2*$^{-/-}$ MEFs is due to the absence of 4E-BPs, and not to some unintended effect of the gene-targeting manipulation, we introduced 4E-BP1 together with 4E-BP2 into *4E-BP1*$^{-/-}$ *4E-BP2*$^{-/-}$

[1]Department of Biochemistry and McGill Cancer Center, McGill University, Montreal, Quebec H3G 1Y6, Canada. [2]Institut de Recherches Cliniques de Montréal, Laboratory of Molecular Immunology, Université de Montréal, Montréal, Quebec H2W 1R7, Canada. [3]Ottawa Health Research Institute, Ottawa, Ontario K1H 8L6, Canada.
*These authors contributed equally to this work.

MEFs. Expression of 4E-BP1 and 4E-BP2, but not empty vector, restored the susceptibility of the *4E-BP1*$^{-/-}$ *4E-BP2*$^{-/-}$ MEFs to VSV infection (Supplementary Fig. 2). These data demonstrate that the virus-resistant phenotype of *4E-BP1*$^{-/-}$ *4E-BP2*$^{-/-}$ MEFs is directly associated with the lack of 4E-BPs.

Next, we investigated whether *4E-BP1*$^{-/-}$ *4E-BP2*$^{-/-}$ MEFs are resistant to infection by other viruses. Wild-type and *4E-BP1*$^{-/-}$ *4E-BP2*$^{-/-}$ MEFs were infected with positive and negative strand RNA viruses, such as Sindbis virus (alphavirus, positive strand), encephalomyocarditis virus (EMCV; picornavirus, positive strand) and influenza virus (orthomyxovirus, negative strand). Similar to VSV (rhabdovirus, negative strand), protein synthesis of Sindbis virus (Supplementary Fig. 3A), EMCV (Supplementary Fig. 3B) and influenza virus (Supplementary Fig. 3C) was severely impaired in *4E-BP1*$^{-/-}$ *4E-BP2*$^{-/-}$, as compared to wild-type, MEFs. Accordingly, a marked reduction (>3,000-fold) in virus titres was observed for all three viruses in *4E-BP1*$^{-/-}$ *4E-BP2*$^{-/-}$ MEFs (Supplementary Fig. 3D). Taken together, these data demonstrate that the lack of 4E-BPs markedly impairs the replication of a broad spectrum of viruses.

Upregulation of type-I IFN response in *4E-BP1*$^{-/-}$ *4E-BP2*$^{-/-}$ MEFs

How do the 4E-BPs affect the replication of disparate viruses? A simple explanation would be that the threshold for eliciting type-I IFN production is lowered in MEFs lacking 4E-BPs. To test this hypothesis, wild-type and *4E-BP1*$^{-/-}$ *4E-BP2*$^{-/-}$ MEFs were treated with poly(I:C), a synthetic double-stranded (ds)RNA that is a potent inducer of type-I IFN. The production of IFN was determined by assessing the inhibition of the VSV-induced cytopathic effect. Six hours after treatment with poly(I:C), culture medium from wild-type and *4E-BP1*$^{-/-}$ *4E-BP2*$^{-/-}$ MEFs was collected and added to wild-type MEFs (Fig. 2a). After overnight incubation, MEFs were infected with VSV (MOI of 0.1 PFU per cell) and virus yield was determined by a plaque assay. Culture medium from wild-type MEFs treated with a low concentration of poly(I:C) (0.1 μg ml^{-1}) failed to protect cells from VSV infection (Fig. 2b). In contrast, no cytopathic effect was observed and virus production was significantly reduced (~200-fold) in wild-type MEFs incubated with the culture medium from *4E-BP1*$^{-/-}$ *4E-BP2*$^{-/-}$ MEFs. Consistent with the notion that the enhanced resistance of the *4E-BP1*$^{-/-}$ *4E-BP2*$^{-/-}$ MEFs to virus infection is due to increased type-I IFN production, incubation with a neutralizing antibody against IFN-β rescued the VSV-resistant phenotype (Supplementary Fig. 4A).

Expression of IFN-α (*Ifna*) and IFN-β (*Ifnb*) mRNAs was more responsive to treatment with either 0.1 μg ml^{-1} (Fig. 2c) or 1 μg ml^{-1} (Supplementary Fig. 4B) of poly(I:C) in *4E-BP1*$^{-/-}$ *4E-BP2*$^{-/-}$ MEFs compared with wild-type MEFs, as determined by reverse transcriptase polymerase chain reaction (RT–PCR). Moreover, the induction of *Ifna* and *Ifnb* mRNA synthesis after VSV infection was greater in *4E-BP1*$^{-/-}$ *4E-BP2*$^{-/-}$ than in wild-type MEFs (Supplementary Fig. 4C). Consistent with these data, poly(I:C) treatment of *4E-BP1*$^{-/-}$ *4E-BP2*$^{-/-}$ MEFs, but not wild-type MEFs, elicited a robust production of IFN-α (Fig. 2d and Supplementary Fig. 5C) and IFN-β (Supplementary Fig. 5A, B), as determined by enzyme-linked immunosorbent assay (ELISA). Collectively, these data show that the lack of 4E-BPs results in enhanced type-I IFN production.

Double knockout mice are protected against VSV infection

To determine whether the virus-resistant phenotype of *4E-BP1*$^{-/-}$ *4E-BP2*$^{-/-}$ MEFs is recapitulated *in vivo*, wild-type and *4E-BP1*$^{-/-}$ *4E-BP2*$^{-/-}$ mice were infected intranasally with VSV (5×10^7 PFU). We chose VSV because its replication is exquisitely sensitive to inhibition by type-1 IFN[17]. By day 6 after infection, 80% of

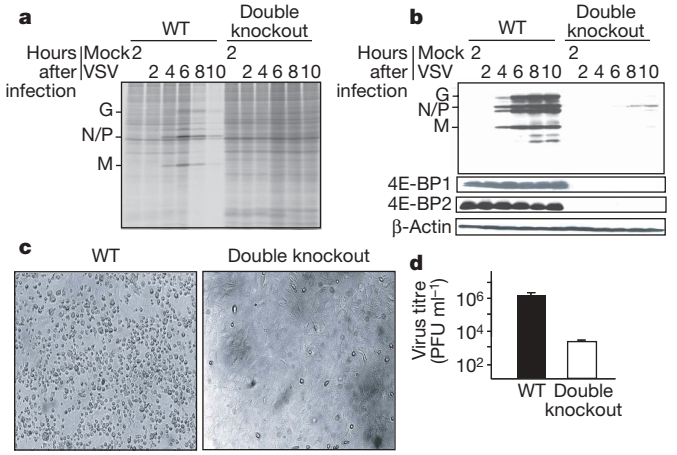

Figure 1 | Lack of 4E-BPs renders MEFs refractory to VSV replication. Wild-type and *4E-BP1*$^{-/-}$ *4E-BP2*$^{-/-}$ MEFs were mock-infected or infected with VSV at an MOI of 0.5 PFU per cell. **a**, MEFs were incubated with [^{35}S]methionine for 30 min at the indicated times after infection. Proteins were subjected to SDS–PAGE (15%). An autoradiogram of the dried gel is shown. Viral proteins are indicated on the left. G, glycoprotein; M, matrix protein; N/P, nucleocapsid protein/phosphoprotein. **b**, Western blotting analysis using antibodies against VSV proteins, 4E-BP1, 4E-BP2 and β-actin. **c**, **d**, Cytopathic effect (**c**) and virus yield (**d**) at 10 h after infection in wild-type and *4E-BP1*$^{-/-}$ *4E-BP2*$^{-/-}$ MEFs (mean ± s.d. of four experiments).

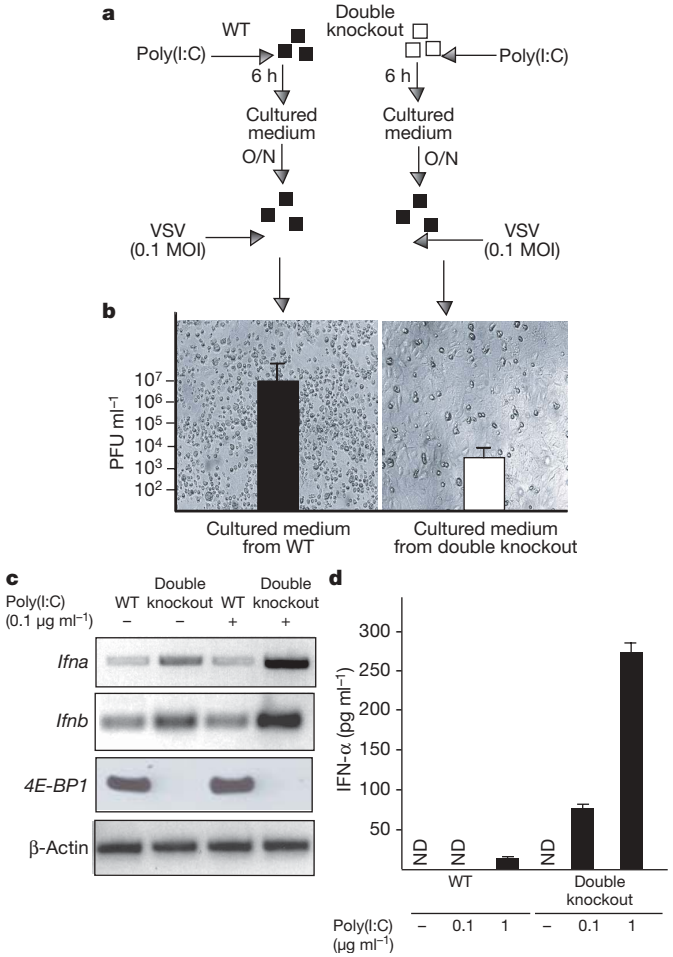

Figure 2 | Enhanced production of type-I IFN in *4E-BP1*$^{-/-}$ *4E-BP2*$^{-/-}$ MEFs. **a**, Diagram of experimental protocol. Wild-type (filled squares) and *4E-BP1*$^{-/-}$ *4E-BP2*$^{-/-}$ (open squares) MEFs were treated with poly(I:C) (0.1 μg ml^{-1}) for 6 h and medium was collected. Wild-type MEFs were incubated overnight (O/N) with the cultured medium from wild-type and *4E-BP1*$^{-/-}$ *4E-BP2*$^{-/-}$ MEFs and then infected with VSV. **b**, Cytopathic effect and virus titres at 24 h after infection. **c**, MEFs were treated with poly(I:C) for 6 h and the induction of *Ifna* and *Ifnb* mRNAs was determined by RT–PCR. **d**, MEFs were treated with poly(I:C) for 6 h and the production of IFN-β was determined by ELISA (mean ± s.d. of three experiments). ND, not detected.

VSV-infected *4E-BP1*$^{-/-}$ *4E-BP2*$^{-/-}$ mice survived, in comparison to 20% of the wild-type mice (Fig. 3a). Furthermore, VSV-infected *4E-BP1*$^{-/-}$ *4E-BP2*$^{-/-}$ mice, in contrast to wild-type mice, failed to exhibit severe respiratory distress. In a second experiment, mice were infected intranasally with VSV (10^5 PFU) and killed 5 days after infection. In lungs from *4E-BP1*$^{-/-}$ *4E-BP2*$^{-/-}$ mice, virus load was reduced (~100-fold; Fig. 3b). The expression of both *Ifna* and *Ifnb* mRNAs, as assayed by RT–PCR, was significantly increased (~3-fold) already by 2 days after infection, as compared to wild-type mice (Fig. 3c). In addition, the serum of VSV-infected *4E-BP1*$^{-/-}$ *4E-BP2*$^{-/-}$ mice contained increased IFN-α levels, as compared to the serum of VSV-infected wild-type mice (Supplementary Fig. 6). Thus, mice lacking 4E-BP1 and 4E-BP2 are resistant to VSV infection and produce more type-I IFN, as compared to wild-type mice.

Plasmacytoid dendritic cells are the main producers of systemic type-I IFN in response to virus infection[18]. To determine whether plasmacytoid dendritic cells from *4E-BP1*$^{-/-}$ *4E-BP2*$^{-/-}$ mice contribute to the virus-resistant phenotype, splenic plasmacytoid dendritic cells were incubated with VSV (MOI of 1 and 10 PFU per cell) for 6 h. Plasmacytoid dendritic cells from *4E-BP1*$^{-/-}$ *4E-BP2*$^{-/-}$ mice generated significantly more (>7-fold) IFN-α, as compared to plasmacytoid dendritic cells from wild-type littermates (Fig. 3d). Similarly, plasmacytoid dendritic cells from *4E-BP1*$^{-/-}$ *4E-BP2*$^{-/-}$ mice, which were co-cultured with synthetic CpG-oligodeoxynucleotides (CpG-ODN), produced more IFN-α (>4-fold) than plasmacytoid dendritic cells from wild-type littermates (Fig. 3e). Thus, the virus-resistant phenotype of *4E-BP1*$^{-/-}$ *4E-BP2*$^{-/-}$ mice correlates with the ability of their plasmacytoid dendritic cells to produce increased amounts of IFN-α in response to virus infection.

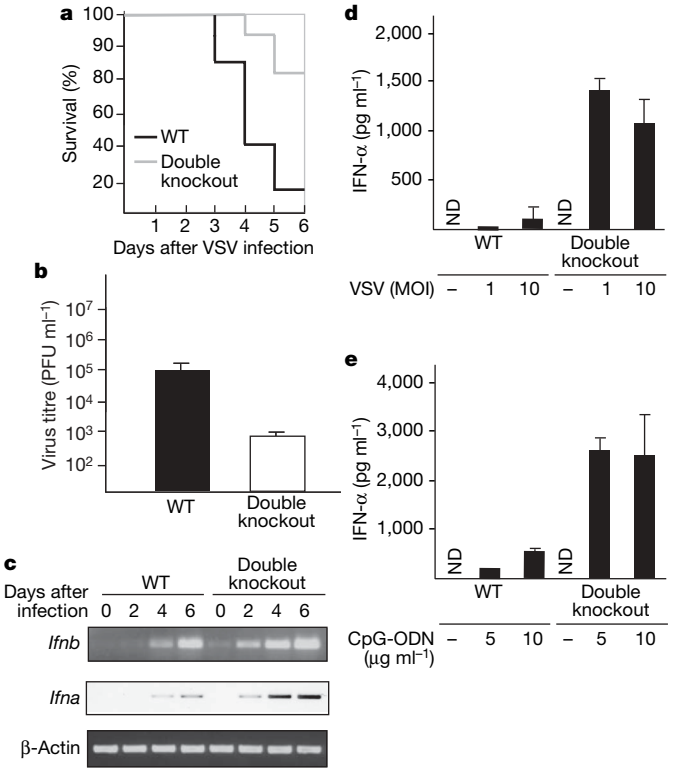

Figure 3 | *4E-BP1*$^{-/-}$ *4E-BP2*$^{-/-}$ mice are resistant to VSV infection. **a**, Mice ($n = 10$) were intransally infected with VSV (5×10^7 PFU) and their survival was plotted as a Kaplan–Meier curve. **b**, Lungs from VSV-infected (10^5 PFU) mice ($n = 3$) were dissected 5 days after infection and virus yield was determined by plaque assay (mean ± s.d.). **c**, Expression of *Ifna* and *Ifnb* genes was determined by RT–PCR in lungs ($n = 3$). **d**, **e**, Splenic plasmacytoid dendritic cells were isolated and cultured for 6 h with VSV (**d**) or incubated overnight in the presence of CpG-ODN (**e**). Secreted IFN-α was measured by ELISA. ND, not detected.

Translational control of *Irf7* mRNA by 4E-BPs

To determine the molecular mechanism by which type-I IFN production is enhanced in *4E-BP1*$^{-/-}$ *4E-BP2*$^{-/-}$ mice, we used gene-expression microarrays. A number of genes in the IFN pathway were upregulated in uninfected *4E-BP1*$^{-/-}$ *4E-BP2*$^{-/-}$ double knockout MEFs as compared to wild-type MEFs (Supplementary Fig. 7A; for a complete list of genes see Supplementary Fig. 7C). Furthermore, a number of genes involved in inflammation and the immune response were also upregulated (Supplementary Fig. 7A).

Because 4E-BPs are translational inhibitors, they are predicted to repress the translation of a subset of mRNAs that are critical for type-I IFN production. To identify these mRNAs, polysomal RNA from wild-type and double knockout MEFs was analysed by gene-expression microarrays. We identified mRNAs with low or no induction at the mRNA level (<1.5-fold), but with a robust induction of translation (>4-fold) (Supplementary Fig. 7B). Notably, *Irf7* mRNA, which encodes the master regulator of the type-I IFN response[19], was the highest ranked gene in this analysis as its expression was increased ~12-fold in *4E-BP1*$^{-/-}$ *4E-BP2*$^{-/-}$ MEFs as compared with wild-type MEFs (Supplementary Fig. 7B).

To validate these results, we studied the recruitment of ribosomes to *Irf7* mRNA using an RT–PCR assay that tracked the polysomal distribution of mRNAs in extracts from wild-type and *4E-BP1*$^{-/-}$ *4E-BP2*$^{-/-}$ MEFs along a sucrose density gradient (Fig. 4a). *Irf7* mRNA was mainly associated with light polysomes in wild-type MEFs (Fig. 4b, left panel), consistent with its inefficient translation initiation. β-Actin mRNA, by contrast, was distributed mainly in heavy polysomes, as expected for an mRNA that is translated efficiently (Fig. 4c). In agreement with the derepression of *Irf7* mRNA translation in *4E-BP1*$^{-/-}$ *4E-BP2*$^{-/-}$ MEFs, the distribution of *Irf7*

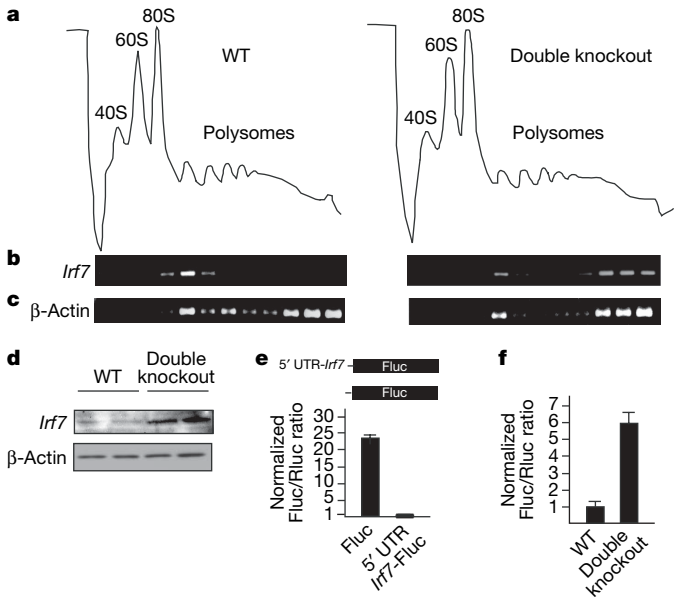

Figure 4 | 4E-BPs inhibit translation of *Irf7* mRNA. **a**, Polysome profiles of wild-type (left) and *4E-BP1*$^{-/-}$ *4E-BP2*$^{-/-}$ (right) MEFs. **b**, **c**, RT–PCR of *Irf7* (**b**) and β-actin (**c**) mRNAs. **d**, Western blot of IRF-7 and β-actin. **e**, Translation of 5′ UTR-*Irf7*-Fluc mRNA (Fluc, top) relative to Fluc mRNA. A *Renilla* luciferase (Rluc) reporter vector was co-transfected with both reporters as a transfection control. Fluc was normalized against Rluc. Values for the Fluc reporter were ~7×10^4 RLU (relative light units) and ~3×10^3 RLU for the 5′ UTR-*Irf7*-Fluc reporter. Rluc values were ~1×10^6 RLU. **f**, Ratio of expression of 5′ UTR-*Irf7*-Fluc/Rluc. The 5′ UTR-*Irf7*-Fluc and Rluc reporters were co-transfected. Fluc activity was normalized against Rluc activity. The Fluc value for wild-type MEFs was set as 1. For wild-type MEFs, Fluc ranged between 1×10^3 and 6×10^3 RLU and Rluc between 1.2×10^6 and 3.4×10^6. For *4E-BP1*$^{-/-}$ *4E-BP2*$^{-/-}$ MEFs, Fluc ranged between 3.5×10^3 and 2.4×10^4 RLU and Rluc between 9×10^5 and 1.5×10^6 RLU.

mRNA was significantly shifted to heavier gradient fractions (Fig. 4b, right panel). Accordingly, in the absence of 4E-BP1 and 4E-BP2, IRF-7 protein amounts were increased (>4-fold), as determined by western blotting (Fig. 4d). These data support a role for the 4E-BPs in the repression of translation of *Irf7* mRNA.

Changes in the 4E-BPs/eIF4E ratio do not alter general translation, but rather affect the translation of a subset of mRNAs that harbour a structured 5′ untranslated region (5' UTR)[7,20]. Notably, the *Irf7* mRNA has a highly structured 5′ UTR that is evolutionarily conserved (data not shown). To examine directly the role of the 5′ UTR in the regulation of *Irf7* mRNA translation, we generated a plasmid vector in which the SV40 promoter drives the expression of the 5′ UTR of *Irf7* mRNA fused to a firefly luciferase (Fluc) reporter (5' UTR-*Irf7*-Fluc; Fig. 4e). As expected, because of the 5′ UTR secondary structure, the expression of 5′ UTR-*Irf7*-Fluc in wild-type MEFs was reduced relative to the control (lacking the 5′ UTR) Fluc reporter. A *Renilla* luciferase (Rluc) reporter plasmid was used as a transfection control (Fig. 4e). Next, wild-type and double knockout MEFs were co-transfected with 5′ UTR-*Irf7*-Fluc and an Rluc reporter plasmid. Consistent with the repression of *Irf7* mRNA translation by 4E-BPs, the normalized Fluc/Rluc ratio was significantly increased (~6-fold) in *4E-BP1*$^{-/-}$ *4E-BP2*$^{-/-}$ MEFs as compared with wild-type MEFs (Fig. 4f). Therefore, we conclude that the *Irf7* mRNA 5′ UTR has a critical role in its translational repression by 4E-BPs.

To determine whether the virus-resistant phenotype and the enhanced type-I IFN production in *4E-BP1*$^{-/-}$ *4E-BP2*$^{-/-}$ MEFs are due to increased IRF-7 expression, we reduced the IRF-7 level in *4E-BP1*$^{-/-}$ *4E-BP2*$^{-/-}$ MEFs using a short hairpin (sh)RNA against *Irf7* mRNA. shRNA against *Irf7* mRNA, but not a control shRNA, restored the sensitivity of these cells to VSV infection and blocked type-I IFN production (Fig. 5). These data provide genetic evidence that the enhanced type-I IFN response in *4E-BP1*$^{-/-}$ *4E-BP2*$^{-/-}$ MEFs is caused by upregulation of IRF-7 expression.

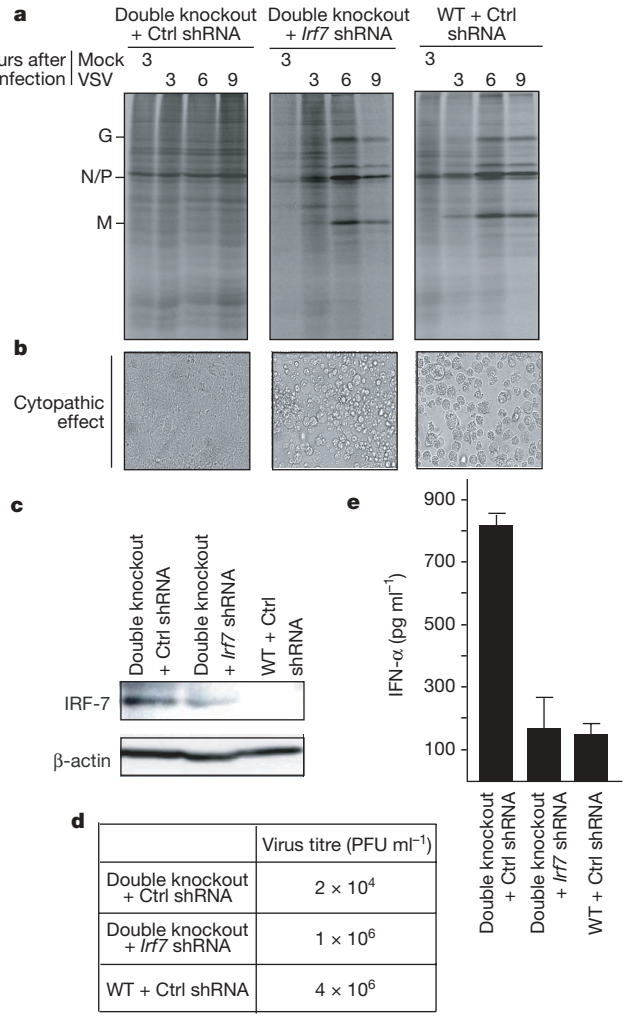

d

	Virus titre (PFU ml^{-1})
Double knockout + Ctrl shRNA	2×10^4
Double knockout + *Irf7* shRNA	1×10^6
WT + Ctrl shRNA	4×10^6

Figure 5 | Reduction of IRF-7 in *4E-BP1*$^{-/-}$ *4E-BP2*$^{-/-}$ MEFs renders the cells susceptible to VSV infection and blocks type-I IFN production. a, *4E-BP1*$^{-/-}$ *4E-BP2*$^{-/-}$ MEFs were first transfected with a control (Ctrl) shRNA or an shRNA against *Irf7* and then infected with VSV (MOI of 1 PFU per cell) and incubated with [^{35}S]methionine. Proteins were analysed by SDS–PAGE (15%). Viral proteins are indicated on the left. **b**, Cytopathic effect was visualized at 9 h after infection. **c**, Western blot analysis using antibodies against IRF-7 and β-actin. **d**, Virus yield was determined at 9 h after infection. **e**, IFN-α was determined 9 h after infection by ELISA (mean ± s.d. of three experiments).

Discussion

Virus infection results in the induction of type-I IFN, which confers an antiviral state on the host cell. New expression of IFN-related genes is required for the activation of the innate immune response[21,22]. The balance between activators and repressors of type-I IFN response is critical for this process. Until now, studies described only positive regulators of the innate immune response. For instance, *Stat1* and *Stat2* knockout mice[23–25] and RNase L (*Rnasel*) knockout mice[26] exhibit increased sensitivity to virus infections because of impaired IFN response. Knockout mice for two virus cytoplasmic sensors, retinoic-acid-inducible gene I (RIG-I) and melanoma differentiation associated gene 5 (MDA5), display a similar phenotype[27,28]. Our results provide new insight into the molecular mechanism of the innate immune response by providing strong evidence for a repressive translational mechanism that impedes type-I IFN production. We show that MEFs lacking 4E-BPs are largely refractory to infection by a variety of viruses (Fig. 1 and Supplementary Fig. 3). The virus-resistant phenotype is due to an increased type-I IFN production, as determined by inhibition of VSV replication, as well as RT–PCR, microarray and ELISA analyses (Fig. 2 and Supplementary Figs 4 and 5). In *4E-BP1*$^{-/-}$ *4E-BP2*$^{-/-}$ double knockout mice VSV replication was suppressed. The VSV-resistant phenotype correlates with enhanced production of IFN-α in plasmacytoid dendritic cells (Fig. 3). These data indicate a causative role of the enhanced expression of type-I IFN in plasmacytoid dendritic cells in the resistance of *4E-BP1*$^{-/-}$ *4E-BP2*$^{-/-}$ mice to VSV infection.

It is thought that plasmacytoid dendritic cells produce large amounts of type-I IFN as a consequence of a high constitutive expression of IRF-7 (ref. 18). Consistent with the control of *Irf7* mRNA translation by 4E-BPs, we demonstrated that the level of 4E-BP1 and 4E-BP2 in plasmacytoid dendritic cells is significantly lower as compared to MEFs (Supplementary Fig. 8). Thus, the low levels of 4E-BPs could explain the constitutive expression of IRF-7 in plasmacytoid dendritic cells.

Other lines of evidence support the idea that downstream targets of mTOR such as 4E-BPs, S6K1/2 or PRAS40 have an important role in repression of IFN production. First, *4E-BP1*$^{-/-}$ MEFs primed with mouse IFN exhibit enhanced expression of IFN-related genes[29]. Second, activation of toll-like receptor 3 (TLR3), which is a major mediator of the cellular response to virus infection through dsRNA, activates phosphatidylinositol-3-OH kinase (PI(3)K), an upstream regulator of 4E-BPs[30]. Interestingly, PI(3)K-γ and PI(3)K-δ knockout mice exhibit a defect in innate immunity[31]. In addition, pharmacological and genetic inhibition of PI(3)K blocks the induction of IFN-stimulated genes by dsRNA[32]. Third, similar to the phenotype of the *4E-BP1*$^{-/-}$ cells, the expression of type-I IFN genes was enhanced in MEFs lacking the mTOR negative regulator, tuberous sclerosis complex 2, when primed with mouse IFN[29].

How do 4E-BPs regulate type-I IFN production? Our model (Supplementary Fig. 9) is based on the translational control of *Irf7* mRNA by the 4E-BPs. *Irf7* mRNA translation is derepressed in *4E-BP1*$^{-/-}$ *4E-BP2*$^{-/-}$ MEFs (Fig. 4) owing to increased amounts of the eIF4F complex. Because of its highly structured 5′ UTR, the translation of *Irf7* mRNA would be extremely sensitive to changes in the

amounts of eIF4F. In agreement with this model, translation of a reporter mRNA harbouring the 5′ UTR of *Irf7* mRNA is enhanced in *4E-BP1*$^{-/-}$ *4E-BP2*$^{-/-}$ MEFs. An increase in IRF-7 expression triggers type-I IFN production, which subsequently evokes a transcriptionally dependent positive feedback regulation of IRF-7 signalling[33,34]. Consistent with this, we showed that the expression of IFN-α and IFN-β is enhanced (Fig. 2 and Supplementary Figs 4 and 5) and IRF-7 levels are upregulated in uninfected *4E-BP1*$^{-/-}$ *4E-BP2*$^{-/-}$ MEFs (Fig. 4 and Supplementary Fig. 7B). Enhanced type-I IFN production in *4E-BP1*$^{-/-}$ *4E-BP2*$^{-/-}$ MEFs seems to be highly dependent on IRF-7, as decreasing IRF-7 levels by shRNA rendered cells susceptible to virus infection and blocked type-I IFN production (Fig. 5). Accordingly, *Irf7*$^{-/-}$ mice exhibit increased susceptibility to virus infection both *in vivo* and *ex vivo* as well as impaired induction of type-I IFN[19]; that is, a phenotype opposite to that of the *4E-BP1*$^{-/-}$ *4E-BP2*$^{-/-}$ mice. The activation of the IRF-7-mediated type-I IFN response induces the expression of RIG-I and MDA5, which triggers the induction of NF-κB, IRF-3 and IRF-7 that co-operate in the production of the antiviral type-I IFN response. As expected from this model, we found enhanced expression of RIG-I and MDA5 proteins in MEFs lacking 4E-BPs (Supplementary Fig. 10).

Our data provide biochemical, genetic and biological evidence that 4E-BPs constitute a critical step in the activation of the innate immune response. These findings raise the intriguing possibility that regulators of translation might serve as therapeutic targets to boost the innate immune response against virus infection.

METHODS SUMMARY

Mice, cell culture and viruses. *4E-BP1*$^{-/-}$ *4E-BP2*$^{-/-}$ double knockout mice have been described previously[15]. MEFs derived from wild-type and *4E-BP1*$^{-/-}$ *4E-BP2*$^{-/-}$ mice were immortalized by sequential passaging[35]. Splenic plasmacytoid dendritic cells were isolated using anti-mPDCA1 magnetic beads. *Ex vivo* virus infection and metabolic labelling were performed as described[36]. Virus titres were determined by a plaque assay[37,38]. *In vivo* virus experiments were performed as described[38].

Polysome profiling. Polysomes were prepared and analysed as described[39]. *Irf7* and β-actin mRNAs were amplified by RT–PCR reactions, which were optimized to measure the exponential phase on the amplification curve.

Microarray analysis. Total or polysomal RNA was isolated from MEFs using Trizol and hybridized to an Affymetrix Mouse430_2 chip. To identify genes upregulated in *4E-BP1*$^{-/-}$ *4E-BP2*$^{-/-}$ MEFs, total RNA samples were analysed using normalization that reduced the range for the fold change (>1.5-fold used as threshold). Translationally upregulated genes were identified by selecting genes whose regulation in total RNA samples was low (<1.5-fold), but their abundance on polysomes was >4-fold.

ELISA. MEFs were transfected with poly(I:C) using the FuGENE 6 transfection reagent according to the manufacturer's protocol (Roche). Murine IFN-α and IFN-β production was detected by ELISA according to the manufacturer's procedure (PBL Biomedical Laboratories).

Plasmid construction, transfection and luciferase assay. The 5′ UTR of mouse *Irf7* mRNA was amplified and cloned into the pGL3 firefly luciferase (Fluc) reporter vector (Promega). MEFs were co-transfected with 5′ UTR-*Irf7*-Fluc and *Renilla* luciferase (Rluc; Promega) as described[36]. Cell extracts were prepared in passive lysis buffer and assayed for Rluc and Fluc activity using a dual-luciferase reporter assay system (Promega). Fluc activity was normalized against Rluc activity, which was used as a transfection control.

Rescue experiments. pBABE-4E-BP1, pBABE-4E-BP2 and empty vector were transfected into phoenix-293-T packaging cells and virus-containing medium was used to infect *4E-BP1*$^{-/-}$ *4E-BP2*$^{-/-}$ MEFs. *4E-BP1*$^{-/-}$ *4E-BP2*$^{-/-}$ MEFs were transfected with PLKO.1-puro-Ctrl-shRNA or PLKO.1-puro-*Irf7*-shRNA as described[36]. Transfected MEFs were selected with puromycin for 1 week.

Full Methods and any associated references are available in the online version of the paper at www.nature.com/nature.

Received 28 November 2007; accepted 25 January 2008.
Published online 13 February 2008.

1. Garcia-Sastre, A. & Biron, C. A. Type 1 interferons and the virus-host relationship: a lesson in detente. *Science* **312,** 879–882 (2006).
2. Katze, M. G., He, Y. & Gale, M. Jr. Viruses and interferon: a fight for supremacy. *Nature Rev. Immunol.* **2,** 675–687 (2002).
3. Kawai, T. & Akira, S. Innate immune recognition of viral infection. *Nature Immunol.* **7,** 131–137 (2006).
4. Meylan, E., Tschopp, J. & Karin, M. Intracellular pattern recognition receptors in the host response. *Nature* **442,** 39–44 (2006).
5. Mathews, M. B., Sonenberg, N. & Hershey, J. W. B. Origins and principles of translational control. In *Translational Control in Biology and Medicine* (eds Mathews, M. B., Sonenberg, N. & Hershey, J. W. B.) 1–40 (Cold Spring Harbor Laboratory Press, Cold Spring Harbor, New York, 2007).
6. Shatkin, A. J. mRNA cap binding proteins: essential factors for initiating translation. *Cell* **40,** 223–224 (1985).
7. Gingras, A. C., Raught, B. & Sonenberg, N. eIF4 initiation factors: effectors of mRNA recruitment to ribosomes and regulators of translation. *Annu. Rev. Biochem.* **68,** 913–963 (1999).
8. Sonenberg, N., Morgan, M. A., Merrick, W. C. & Shatkin, A. J. A polypeptide in eukaryotic initiation factors that crosslinks specifically to the 5′-terminal cap in mRNA. *Proc. Natl Acad. Sci. USA* **75,** 4843–4847 (1978).
9. Rozen, F. *et al.* Bidirectional RNA helicase activity of eucaryotic translation initiation factors 4A and 4F. *Mol. Cell. Biol.* **10,** 1134–1144 (1990).
10. Pestova, T. V., Lorsch, J. R. & Hellen, C. U. T. In *Translational Control in Biology and Medicine* (eds Mathews, M. B., Sonenberg, N. & Hershey, J. W. B.) 87–128 (Cold Spring Harbor Laboratory Press, Cold Spring Harbor, New York, 2007).
11. Pause, A. *et al.* Insulin-dependent stimulation of protein synthesis by phosphorylation of a regulator of 5′-cap function. *Nature* **371,** 762–767 (1994).
12. Poulin, F., Gingras, A. C., Olsen, H., Chevalier, S. & Sonenberg, N. 4E–BP3, a new member of the eukaryotic initiation factor 4E-binding protein family. *J. Biol. Chem.* **273,** 14002–14007 (1998).
13. Hay, N. & Sonenberg, N. Upstream and downstream of mTOR. *Genes Dev.* **18,** 1926–1945 (2004).
14. Mohr, I. J., Pe'ery, T. & Mathews, M. B. Protein synthesis and translational control during viral infection. In *Translational Control in Biology and Medicine* (eds Mathews, M. B., Sonenberg, N. & Hershey, J. W. B.) 545–600 (Cold Spring Harbor Laboratory Press, Cold Spring Harbor, New York, 2007).
15. Le Bacquer, O. *et al.* Elevated sensitivity to diet-induced obesity and insulin resistance in mice lacking 4E–BP1 and 4E–BP2. *J. Clin. Invest.* **117,** 387–396 (2007).
16. Poulin, F., Brueschke, A. & Sonenberg, N. Gene fusion and overlapping reading frames in the mammalian genes for 4E–BP3 and MASK. *J. Biol. Chem.* **278,** 52290–52297 (2003).
17. Belkowski, L. S. & Sen, G. C. Inhibition of vesicular stomatitis viral mRNA synthesis by interferons. *J. Virol.* **61,** 653–660 (1987).
18. Colonna, M., Trinchieri, G. & Liu, Y. J. Plasmacytoid dendritic cells in immunity. *Nature Immunol.* **5,** 1219–1226 (2004).
19. Honda, K. *et al.* IRF-7 is the master regulator of type-I interferon-dependent immune responses. *Nature* **434,** 772–777 (2005).
20. Koromilas, A. E., Lazaris-Karatzas, A. & Sonenberg, N. mRNAs containing extensive secondary structure in their 5′ non-coding region translate efficiently in cells overexpressing initiation factor eIF-4E. *EMBO J.* **11,** 4153–4158 (1992).
21. Honda, K., Takaoka, A. & Taniguchi, T. Type I interferon [corrected] gene induction by the interferon regulatory factor family of transcription factors. *Immunity* **25,** 349–360 (2006).
22. Stetson, D. B. & Medzhitov, R. Type I interferons in host defense. *Immunity* **25,** 373–381 (2006).
23. Durbin, J. E., Hackenmiller, R., Simon, M. C. & Levy, D. E. Targeted disruption of the mouse Stat1 gene results in compromised innate immunity to viral disease. *Cell* **84,** 443–450 (1996).
24. Meraz, M. A. *et al.* Targeted disruption of the Stat1 gene in mice reveals unexpected physiologic specificity in the JAK-STAT signaling pathway. *Cell* **84,** 431–442 (1996).
25. Park, C., Li, S., Cha, E. & Schindler, C. Immune response in Stat2 knockout mice. *Immunity* **13,** 795–804 (2000).
26. Zhou, A. *et al.* Interferon action and apoptosis are defective in mice devoid of 2′,5′-oligoadenylate-dependent RNase L. *EMBO J.* **16,** 6355–6363 (1997).
27. Kato, H. *et al.* Cell type-specific involvement of RIG-I in antiviral response. *Immunity* **23,** 19–28 (2005).
28. Kato, H. *et al.* Differential roles of MDA5 and RIG-I helicases in the recognition of RNA viruses. *Nature* **441,** 101–105 (2006).
29. Kaur, S. *et al.* Regulatory effects of mammalian target of rapamycin-activated pathways in type I and II interferon signaling. *J. Biol. Chem.* **282,** 1757–1768 (2007).
30. Sarkar, S. N. *et al.* Novel roles of TLR3 tyrosine phosphorylation and PI3 kinase in double-stranded RNA signaling. *Nature Struct. Mol. Biol.* **11,** 1060–1067 (2004).
31. Vanhaesebroeck, B., Ali, K., Bilancio, A., Geering, B. & Foukas, L. C. Signalling by PI3K isoforms: insights from gene-targeted mice. *Trends Biochem. Sci.* **30,** 194–204 (2005).
32. Sen, G. C. & Sarkar, S. N. Transcriptional signaling by double-stranded RNA: role of TLR3. *Cytokine Growth Factor Rev.* **16,** 1–14 (2005).

33. Hiscott, J. *et al.* Convergence of the NF-κB and interferon signaling pathways in the regulation of antiviral defense and apoptosis. *Ann. NY Acad. Sci.* **1010,** 237–248 (2003).
34. Honda, K. & Taniguchi, T. IRFs: master regulators of signalling by Toll-like receptors and cytosolic pattern-recognition receptors. *Nature Rev. Immunol.* **6,** 644–658 (2006).
35. Todaro, G. J. & Green, H. Quantitative studies of the growth of mouse embryo cells in culture and their development into established lines. *J. Cell Biol.* **17,** 299–313 (1963).
36. Costa-Mattioli, M., Svitkin, Y. & Sonenberg, N. La autoantigen is necessary for optimal function of the poliovirus and hepatitis C virus internal ribosome entry site *in vivo* and *in vitro*. *Mol. Cell. Biol.* **24,** 6861–6870 (2004).
37. Berlanga, J. J. *et al.* Antiviral effect of the mammalian translation initiation factor 2α kinase GCN2 against RNA viruses. *EMBO J.* **25,** 1730–1740 (2006).
38. Stojdl, D. F. *et al.* The murine double-stranded RNA-dependent protein kinase PKR is required for resistance to vesicular stomatitis virus. *J. Virol.* **74,** 9580–9585 (2000).
39. Costa-Mattioli, M. *et al.* eIF2α phosphorylation bidirectionally regulates the switch from short- to long-term synaptic plasticity and memory. *Cell* **129,** 195–206 (2007).

Supplementary Information is linked to the online version of the paper at www.nature.com/nature.

Acknowledgements We thank M. Karin, M. Gale, R. Lin, W. Sossin, L. W. Ler and A. Rosenfeld for comments on the paper, and N. Taheri, A. Sylvestre and C. Lister for assistance. RIG-I and MDA5 antibodies were provided by H. Kato. This work was supported by a grant from the National Cancer Institute of Canada to N.S. and J.C.B. N.S. is a Howard Hughes Medical Institute (HHMI) International scholar. R.C. is supported by a Cole Foundation post-doctoral fellowship and R.J.O.D. is supported by a Terry Fox Foundation studentship.

Author Information Reprints and permissions information is available at www.nature.com/reprints. Correspondence and requests for materials should be addressed to N.S. (nahum.sonenberg@mcgill.ca) or M.C.-M. (mauro.costa-mattioli@mail.mcgill.ca).

METHODS

Mice and cell culture. *4E-BP1*$^{-/-}$ *4E-BP2*$^{-/-}$ mice have been described previously[15]. MEFs derived from wild-type and *4E-BP1*$^{-/-}$ *4E-BP2*$^{-/-}$ mice were immortalized by sequential passaging[35]. All experiments were performed at least three times and repeated with independently derived MEFs. Splenic plasmacytoid dendritic cells were isolated using anti-mPDCA1 (murine plasmacytoid dendritic cell antigen-1) magnetic beads according to the manufacturer's instructions (Miltenyi Biotech). The IFN neutralization experiment was performed using a monoclonal antibody against mouse IFN-β according to the manufacturer's procedure (PBL Biomedical Laboratories).

Viruses. The Indiana serotype of VSV was previously described[40]. Influenza virus A/HK/1/68-MA20 was provided by E. G. Brown, EMCV K-2 by V. Agol, and Sindbis virus by J. Berlanga. EMCV, Sindbis virus and VSV were propagated in BHK21 cells. *Ex vivo* virus infection and metabolic labelling were performed as described[36]. Virus titres were determined by a standard plaque assay method[37,38]. For *in vivo* experiments, mice were infected intranasally with VSV and killed 5 days after infection. Lungs were aseptically removed and snap-frozen in liquid nitrogen. Specimens were homogenized in 3 ml of PBS on ice, and titres were determined in BHK21 cells[38].

RT–PCR and RNA extractions. Total RNA was extracted using Trizol reagent (Invitrogen) according to the manufacturer's instructions. Total RNA (1 μg) was reverse transcribed (RT) with Superscript III reverse transcriptase (Invitrogen) for 1 h at 50 °C using oligodT. One microlitre of RT template was incubated with specific primers (described below) and with Taq Polymerase (Fermentas) according to the supplier's instructions. The number of PCR cycles ranged from 23 to 34 depending on the linearity of the reaction. PCR primers included (5′ to 3′): IFN-α sense (CCTTCCACAGGATCACTGTGTACCT), IFN-α antisense (TTCTGCTCTGACCACCTCCC); IFN-β sense (CACAGCCCTCTCCATCAACT), IFN-β antisense (TCCCACGTCAATCTTTCCTC); IRF-7 sense (ATGATGGTCACATCCAGGAACCCA), IRF-7 antisense (TCAGGTCTGCAGTACAGCCACAT); β-actin sense (GGACTCCT ATGTGGGTGACGAGG), β-actin antisense (GGGAGAGCATAGCCCTCGTAGAT). PCR reactions were optimized to measure the exponential phase on the amplification curve.

Polysome profiling. MEFs were washed twice with cold PBS containing 100 μg ml^{-1} cycloheximide, suspended in lysis buffer (5 mM Tris-HCl, pH 7.5, 2.5 mM $MgCl_2$, 1.5 mM KCl, 100 μg ml^{-1} cycloheximide, 2 mM dithiothreitol, 0.5% Triton X-100 and 0.5% sodium deoxycholate), and centrifuged for 2 min at 14,000*g* (Eppendorf centrifuge). The supernatant was loaded onto a 10–50% sucrose gradient prepared in 20 mM HEPES-KOH, pH 7.6, 100 mM KCl and 5 mM $MgCl_2$ and centrifuged at 35,000 r.p.m. for 2 h at 4 °C in an SW40 rotor. Fractions were collected by piercing the tube with a Brandel tube piercer, passing 60% sucrose through the bottom of the tube, followed by monitoring the absorbance using an ISCO UA-6 UV Detector. RNA was isolated from individual fractions using Trizol reagent (Invitrogen).

Microarray analysis. Total RNA or polysomal RNA was isolated from wild-type and *4E-BP1*$^{-/-}$ *4E-BP2*$^{-/-}$ MEFs using Trizol. RNA samples were purified using the Qiagen RNeasy kit (according to the manufacturer's instructions; Qiagen) followed by sodium acetate/ethanol precipitation. Twenty micrograms of each RNA sample were processed according to the manufacturer's protocol (Affymetrix) and hybridized to an Affymetrix Mouse430_2 chip. Primary image analysis of the arrays was performed using the Genechip 3.2 software package (Affymetrix). The data were normalized using Robust Multichip Averaging (RMA)[41] using updated probe set definitions 'REFSEQ_8'[42,43]. RMA leads to a reduced dynamic range of obtained fold changes and hence a moderate threshold was used. To identify genes upregulated in *4E-BP1*$^{-/-}$ *4E-BP2*$^{-/-}$ MEFs, total RNA samples were analysed using normalization that reduced the range for the fold change (>1.5-fold used as threshold).

Translationally upregulated genes were identified by selecting genes whose regulation in total RNA samples was low (<1.5-fold), but their abundance on polysomes was >4-fold (by calculating the ratio between the translational microarray and the total gene expression microarray and then comparing between *4E-BP1*$^{-/-}$ *4E-BP2*$^{-/-}$ and wild-type MEFs). Genes that were related to inflammation or IFN responses were identified manually using information from the Gene Ontology Consortium[44].

Western blot analysis. MEFs were homogenized in buffer A (50 mM Tris-HCl, pH 7.4, 100 mM NaCl, 1% Triton X-100, 1 mM EDTA, 1 mM dithiothreitol, protease inhibitors cocktail (Roche), 20 mM β-glycerophosphate, 0.25 mM Na_3VO_4, 10 mM NaF, 10 nM okadaic acid, 1 mM PMSF) and incubated for 30 min at 4 °C. Cell debris was removed by centrifugation at 10,000*g* (Eppendorf centrifuge) for 10 min at 4 °C and total protein content was determined using a Bio-Rad assay. Laemmli sample buffer was added to the supernatant, which was then subjected to SDS–PAGE (15%). Proteins were transferred onto a nitrocellulose membrane, which was blocked for 2 h at room temperature with 5% skim milk in PBS containing 0.2% Tween 20 (PBS-T) and washed twice with PBS-T. The membrane was incubated overnight at 4 °C with primary antibodies followed by three 10-min washes in PBS-T and further incubated with peroxidase-coupled secondary antibody for 30 min at room temperature, and washed three times. Detection of peroxidase-coupled secondary antibody was performed with ECL (GE-Healthcare).

RIG-I and MDA5 antibodies were provided by H. Kato. IRF-7 antibody was purchased from Santa Cruz Biotechnology.

ELISA. MEFs were transfected with poly(I:C) using FuGENE 6 transfection reagent (Roche) according to the manufacturer's protocol. Cultured medium was recovered at 3 h and 6 h after transfection. Murine IFN-α and IFN-β production was detected in the cultured medium by ELISA according to the manufacturer's procedure (PBL Biomedical Laboratories).

Plasmid construction, transfection and luciferase assay. A 411-bp DNA corresponding to the 5′ UTR of mouse *Irf7* mRNA was amplified by PCR from MEF genomic DNA. HindIII and NcoI restriction sites were added to the 5′ and 3′ ends, respectively. Using the same restriction sites, the *Irf7* 5′ UTR was cloned into the pGL3 firefly luciferase (Fluc) reporter vector (Promega). MEFs were co-transfected with 500 ng of 5′ UTR-*Irf7*-Fluc and 100 ng of *Renilla* luciferase (Rluc; Promega) vector, which is under the control of the CMV promoter, in 24-well plates using Lipofectamine 2000 as described[36]. Cell extracts were prepared in passive lysis buffer (Promega) 20 h after transfection and assayed for Rluc and Fluc activity in a Lumat LB9507 bioluminometer (EG&G Bertold) using a dual-luciferase reporter assay system (Promega), according to the manufacturer's instructions. Fluc activity was normalized against Rluc activity, which was used as a transfection control.

Rescue experiments. pBABE-4E-BP1, pBABE-4E-BP2 and empty vector constructs were transfected into phoenix-293-T packaging cells. After 48 h, virus-containing medium was filtered, collected and used to infect *4E-BP1*$^{-/-}$ *4E-BP2*$^{-/-}$ MEFs in the presence of 5 mg ml^{-1} of polybrene (Sigma-Aldrich). Cells were re-infected the next day and supplemented with puromycin (2 μg ml^{-1}, Sigma-Aldrich) for selection for five days.

shRNA against *Irf7*. *4E-BP1*$^{-/-}$ *4E-BP2*$^{-/-}$ MEFs were transfected with PLKO.1-puro-Ctrl-shRNA (CAACAAGATGAAGAGCACCAA; Origene) or PLKO.1-puro-*Irf7*-shRNA (GTCACCACACTACACCATCTA; Origene) as described[36]. Transfected MEFs were selected with puromycin for 1 week.

40. Stojdl, D. F. *et al.* Exploiting tumor-specific defects in the interferon pathway with a previously unknown oncolytic virus. *Nature Med.* **6,** 821–825 (2000).
41. Irizarry, R. A. *et al.* Summaries of Affymetrix GeneChip probe level data. *Nucleic Acids Res.* **31,** e15 (2003).
42. Dai, M. *et al.* Evolving gene/transcript definitions significantly alter the interpretation of GeneChip data. *Nucleic Acids Res.* **33,** e175 (2005).
43. Sandberg, R. & Larsson, O. Improved precision and accuracy for microarrays using updated probe set definitions. *BMC Bioinformatics* **8,** 48 (2007).
44. Gene Ontology Consortium.. The Gene Ontology (GO) project in 2006. *Nucleic Acids Res.* **34,** D322–D326 (2006).